Published by
NIGERIAN SOCIETY OF PHYSICAL SCIENCES
Available online @ https://journal.nsps.org.ng/index.php/jnsps

J. Nig. Soc. Phys. Sci. 7 (2025) 2572

Journal of the Nigerian Society of Physical Sciences

Optimal control strategies for dynamical model of climate change under real data

Fatmawati[a,*], Faishal F. Herdicho[a], Nurina Fitriani[b], Norma Alias[c], Mazlan Hashim[d], Olumuyiwa J. Peter[e,f,g]

[a]*Department of Mathematics, Faculty of Science and Technology, Universitas Airlangga, Surabaya, Indonesia*
[b]*Department of Biology, Faculty of Science and Technology, Universitas Airlangga, Surabaya, Indonesia*
[c]*Department of Mathematical Sciences, Faculty of Science, Universiti Teknologi Malaysia, Johor Bahru, Johor, Malaysia*
[d]*Geoscience & Digital Earth Centre (INSTEG), Research Institute for Sustainable Environment (RISE), Universiti Teknologi Malaysia, Johor Bahru, Johor, Malaysia*
[e]*Department of Mathematics, Saveetha School of Engineering, SIMATS, Saveetha University, Chennai, Tamil Nadu, 602105, India*
[f]*Department of Mathematical and Computer Sciences, University of Medical Sciences, Ondo City, Ondo State, Nigeria*
[g]*Department of Epidemiology and Biostatistics, School of Public Health, University of Medical Sciences, Ondo City, Ondo State, Nigeria*

Abstract

Climate change is primarily caused by increasing levels of carbon dioxide (CO_2) in the atmosphere, with significant impacts on global temperatures and ecosystems. The interplay between CO_2 levels, forest biomass, and temperature highlights how important it is to conserve these vital ecosystems in order to effectively combat climate change. In this study, we construct and analyze the Lotka-Volterra model to explore the interactions between concentration of CO_2, photosynthetic biomass density and atmospheric temperature. The results of the model analysis obtained four locally asymptotically stable equilibria under specific conditions and two unstable equilibria. Based on the results of the sensitivity analysis, the most influential parameters affecting changes in concentration number are intrinsic rate of accumulation of CO_2 and natural reduction rate of CO_2. Next to estimate the model parameters, we employ the least-squares method, enabling us to apply the model to actual temperature data from Surabaya city, Indonesia. The numerical simulation results show that CO_2 concentration is expected to range from 400 to 420 ppm, biomass density is estimated to be between 92 and 102 kg/m^3, and atmospheric temperature is projected around 28.1^{o}C −29.1^{o}C. Next, using the Incremental Cost-Effectiveness Ratio (ICER) calculation, implementing control strategy in the form of limiting access to private vehicles and reforestation is the best strategy to make the temperature better and cost efficiency.

DOI:10.46481/jnsps.2025.2572

Keywords: Climate change, cost-effectiveness analysis, mathematical model, optimal control, parameters estimation

Article History :
Received: 17 December 2024
Received in revised form: 26 March 2025
Accepted for publication: 29 April 2025
Available online: 21 May 2025

© 2025 The Author(s). Published by the Nigerian Society of Physical Sciences under the terms of the Creative Commons Attribution 4.0 International license. Further distribution of this work must maintain attribution to the author(s) and the published article's title, journal citation, and DOI.

Communicated by: P. Thakur

1. Introduction

Climate change is primarily caused by increasing levels of carbon dioxide (CO_2) in the atmosphere, with significant impacts on global temperatures and ecosystems [1, 2]. Air pollution is also a main contributor to climate change, which exacerbates threats to human health [3]. Fossil fuel burning and deforestation contribute significantly to increasing CO2 levels, which in turn leads to rising temperatures and changing weather patterns [1]. Forest biomass, which includes trees and other vegetation, plays a crucial role in regulating the Earth's climate

*Corresponding author Tel. No.: +91-772-592-2864.
Email address: fatmawati@fst.unair.ac.id (Fatmawati)

by absorbing CO_2 through photosynthesis and storing it in their biomass [4]. However when forest are cut down or degraded, the carbon stored in the trees is released into the atmosphere, not only increasing CO_2 but also contributing to further warming. The interplay between CO_2 levels, forest biomass, and temperature highlights how important it is to conserve these vital ecosystems in order to effectively combat climate change [5].

Surabaya as the 2^{nd} largest city in Indonesia plays an important role in economic and environmental development at the national level. Industries in Surabaya such as the food industry, transportation, households, and population tend to increase every year. The existence of industrial areas in the Surabaya city results in high production of motor vehicles, industrial activities, and increasing demand for high population needs. One of them is in the transportation sector which has very dense activity in Surabaya city [6]. This can increase the level of air pollution and can have an impact on increasing air temperatures in Surabaya city. The lowest air quality is the presence of CO_2 emissions. With increasing levels of CO_2 in the atmosphere, global warming will occurs. This is a challenge for the Surabaya city in managing the impacts of climate change for further study [7].

Mathematical model is a tool for understanding population dynamics that we can apply to temperature change models. Hence, it possible to predict and manage temperature in the environment. In addition, the availability of environmental temperature data will improve model parameter estimates, allowing mathematical models to explain temperature changes in a region using these parameter values. Various authors have formulated climate change models by combining optimal control variables to examine effective intervention strategies. The main aim of the optimal control strategy in a climate change model is to reduce environmental temperature.

Several researchers have studied the dynamics of climate changes. Biswas *et al*. [8] studied a mathematical model of climate change and apply optimal control techniques in the form of greenhouse gases (GHGs). Mandal *et al*. [9] learned a mathematical model to discuss the effect of GHGs on climate change increasing atmospheric temperature and their combined harmful effect on living beings near coastal areas. Kurniawan *et al*. [10] analyzed a mathematical model of global warming effect on the melting of polar ice caps with variables control of clean technology and reforestation. Ref. [11] considered a mathematical model to examine the impact of rapid GHG emissions on climate change and coastal ecosystems involving two control strategies: coastal green belts and desulfurization. Soldatenko *et al*. [12] developed stochastic climate models and their application for the exploration of climate variability by taking into account the dependence of human health on environmental conditions.

Din *et al*. [13] constructed a mathematical model of climate change using the fractional derivative. Achimugwu *et al*. [14] explored a dynamical system involving photosynthetic biomass density, good conservation policies, illumination programs, and direct air capture technology. Sangwan *et al*. [15] presented a mathematical model to estimate the need for green open space based on land surface temperature reduction. Ref. [16] addressed a mathematical model for determining the conditions under which the rate of increase in the concentration of greenhouse gases (GHG) in the atmosphere by combining economic sectors in a holistic structure. Ochieng [17] studied a mathematical model for predicting future climate trends. Shahid *et al*. [18] analyzed the trend of carbon dioxide CO2 emissions in Pakistan between 1990 and 2020 to effectively model dynamics of carbon emissions. Ref. [19] used machine learning model for air pollution prediction and an air quality index classification process during the pandemic.

In this work, we develop a Lotka-Volterra model to explore the interactions between CO2 concentration, photosynthetic biomass density, and atmospheric temperature. The model formulation is presented in Section 2.1. The stability analysis of the equilibria is done in Section 2.2. The calculation of the concentration number as a threshold quantity represents a critical level of CO_2 concentration in the atmosphere, as discussed in Section 2.3. Next, we estimate the model parameters to investigate the dynamics of temperature changes using monthly temperature data in Surabaya, Indonesia from 2020 to 2022 using the least-square fitting technique in Section 3.1. To identify the parameters that influence the model, we conduct an analysis in Section 3.2. Section 3.3 presents the model simulations to examine future climate trends and their potential environmental implications. Additionally, the optimal control problem that takes into account the allowable controls in the form of limiting access to private vehicles and reforestation which continued with the completion of optimal control and numerical simulations of the optimal control model is devoted in Section 3.4. Furthermore, in Section 3.5 we present the cost analysis calculation to identify the best optimal control strategy. Finally, Section 4 concludes the paper.

2. The Model

2.1. Model formulation

Here, the Lotka-Volterra model of interaction between concentration of CO_2 (C), photosynthetic biomass density (B) and atmospheric temperature (T) is explained. The Lotka-Volterra model is a system of differential equations commonly utilized to describe interacting populations. The following are some of the assumptions in constructing the model.

- All the model parameters are non-negative.
- The intrinsic growth of biomass density follows a logistic growth pattern.
- Carbon dioxide (CO_2) is absorbed by biomass in the photosynthesis process.
- Carbon dioxide (CO_2) causes the increase of atmospheric temperature follows Holling type 2 functional response.
- Biomass causes the decrease of atmospheric temperature follows Holling type 2 functional response.

Table 1: Parameters description.

Parameter	Description
α_1	Intrinsic rate of accumulation of CO_2
α_2	Photosynthetic biomass growth rate
α_3	Exothermic heating rate
δ_1	Reduction rate of CO_2 by forest biomass activity
δ_2	Warming-induced CO_2 accumulation rate
σ_1	CO_2 absorption rate for photosynthesis
σ_2	Warming-induced biomass loss rate
θ_1	CO_2-driven warming rate
θ_2	Photosynthetic heat absorption rate
μ_1	Natural reduction rate of CO_2
μ_2	Natural decline rate of biomass
μ_3	Natural decline rate in air temperature
K_B	Carrying capacity of forest ecosystem
γ_1, γ_2	Half saturation constants

We use the Holling Type 2 to illustrates that the temperature will decrease if CO_2 is absorbed by biomass and will be constant if the biomass reaches the saturation point in absorption.

Based on the assumptions, the mathematical model of temperature change by three-dimensional nonlinear autonomous system of ordinary differential equations is presented as.

$$\begin{aligned}\frac{dC}{dt} &= \alpha_1 C - \delta_1 CB + \delta_2 CT - \mu_1 C,\\ \frac{dB}{dt} &= \alpha_2 B\left(1 - \frac{B}{K_B}\right) + \sigma_1 CB - \sigma_2 BT - \mu_2 B,\\ \frac{dT}{dt} &= \alpha_3 T + \frac{\theta_1 CT}{T+\gamma_1} - \frac{\theta_2 BT}{T+\gamma_2} - \mu_3 T,\end{aligned} \tag{1}$$

subject to the initial conditions by $C(0) > 0$, $B(0) > 0$ and $T(0) > 0$, with the solutions of system (1) remain non-negative for all time $t > 0$ and bounded to $C(t) > 0$, $0 < B(t) \leq K_B$ and $T(t) > 0$.

The description of the parameters is given in Table 1.

2.2. Analytical analysis of the model

In this section, we examines the mathematical properties of model (1) for deeper understanding of the model's behavior. The analysis focuses on determine the equilibrium points with its condition of existence and the local stability analysis of equilibrium points.

2.2.1. The equilibrium points of the model

The equilibrium points of the system (1) are obtained by equating the right-hand sides to zero and solving for the state variables. Then, we find six equilibrium points as follows.

a. Equilibrium point for extinction of the entire state. The equilibrium point for extinction of the entire state is as follows.

$$E_0 = (C_0, B_0, T_0) = (0, 0, 0). \tag{2}$$

b. Equilibrium point of biomass existence. The equilibrium point for existence of biomass is as follows.

$$E_1 = (C_1, B_1, T_1) = \left(0, \frac{K_B(\alpha_2 - \mu_2)}{\alpha_2}, 0\right). \tag{3}$$

This equilibrium exist if $\alpha_2 > \mu_2$.

c. Equilibrium point of CO_2 and biomass existence. The equilibrium point for existence of CO_2 and biomass is as follows.

$$\begin{aligned}E_2 &= (C_2, B_2, T_2)\\ &= \left(\frac{K_B\delta_1(\mu_2 - \alpha_2) + \alpha_2(\alpha_1 - \mu_1)}{K_B\delta_1\sigma_1}, \frac{\alpha_1 - \mu_1}{\delta_1}, 0\right).\end{aligned} \tag{4}$$

This equilibrium exist if $\alpha_1 > \mu_1$ and $\mu_2 > \alpha_2$.

d. Equilibrium point of CO_2 and temperature existence. The equilibrium point for existence of CO_2 and temperature is as follows.

$$E_3 = (C_3, 0, T_3), \tag{5}$$

with,

$$\begin{aligned}C_3 &= \frac{\delta_2\gamma_1(\mu_3 - \alpha_3) + (\mu_1 - \alpha_1)(\mu_3 - \alpha_3)}{\delta_2\theta_1},\\ T_3 &= \frac{\mu_1 - \alpha_1}{\delta_2}.\end{aligned}$$

This equilibrium exist if $\mu_1 > \alpha_1$ and $\mu_3 > \alpha_3$.

e. Equilibrium point of biomass and temperature existence. The equilibrium point for existence of biomass and temperature is as follows.

$$E_4 = (0, B_4, T_4), \tag{6}$$

with,

$$\begin{aligned}B_4 &= \frac{K_B(\alpha_3 - \mu_3)(\gamma_2\sigma_2 + \alpha_2 - \mu_2)}{K_B\sigma_2\theta_2 + \alpha_2(\alpha_3 - \mu_3)},\\ T_4 &= \frac{K_B\theta_2(\alpha_2 - \mu_2) + \alpha_2\gamma_2(\mu_3 - \alpha_3)}{K_B\sigma_2\theta_2 + \alpha_2(\alpha_3 - \mu_3)}.\end{aligned}$$

This equilibrium exist if $\alpha_2 > \mu_2$, $\alpha_3 > \mu_3$, and $K_B\theta_2(\alpha_2 - \mu_2) > \alpha_2\gamma_2(\mu_3 - \alpha_3)$.

f. Equilibrium points of co-existence. The equilibrium points of co-existence are as follows.

$$E_5 = (C_5, B_5, T_5), \tag{7}$$

with,

$$\begin{aligned}C_5 &= \frac{\alpha_2\delta_2}{K_B\delta_1\sigma_1}T_5 + \alpha_2(\alpha_1 - \mu_1),\\ B_5 &= \frac{1}{\sigma_1}(\sigma_2 T_5 + \mu_2 - \alpha_2) + \frac{1}{K_B\delta_1\sigma_1}(\delta_2\alpha_2 T_5 + \alpha_2(\alpha_1 - \mu_1)),\end{aligned}$$

and T_5 are the roots of the following equation.

$$a_1 T_5^2 + a_2 T_5 + a_3 = 0, \tag{8}$$

with,

$$\begin{aligned}
a_1 &= K_B\delta_1\sigma_1(\mu_3-\alpha_3) + K_B(\delta_2\sigma_1\theta_2 - \delta_1\sigma_2\theta_1) - \alpha_2\delta_2\theta_1,\\
a_2 &= K_B\delta_1\sigma_1\gamma_1(\mu_3-\alpha_3) + K_B\delta_1\sigma_1\gamma_2(\mu_3-\alpha_3)\\
&\quad + K_B\sigma_1\theta_2(\alpha_1-\mu_1) + K_B\delta_1\theta_1(\alpha_2-\mu_2)\\
&\quad + K_B(\delta_2\sigma_1\theta_2\gamma_1 - \delta_1\sigma_2\theta_1\gamma_2) + \alpha_2\theta_1(\mu_1-\alpha_1)\\
&\quad - \alpha_2\delta_2\theta_1\gamma_2,\\
a_3 &= K_B\delta_1\sigma_1\gamma_1\gamma_2(\mu_3-\alpha_3) + K_B\sigma_1\theta_2\gamma_1(\alpha_1-\mu_1)\\
&\quad + K_B\delta_1\theta_1\gamma_2(\alpha_2-\mu_2) + \alpha_2\gamma_2\theta_1(\mu_1-\alpha_1).
\end{aligned}$$

Then, the equation (8) has one positive real root number if $\alpha_1 > \mu_1, \mu_2 > \alpha_2$, and either $a_1 > 0, a_3 > 0$ or $a_1 < 0, a_3 < 0$.

2.2.2. *Local stability analysis*

After obtaining the equilibrium points in the section (2.2.1), in this section the local stability of each equilibrium points will be analyzed. First, we linearization model (1). The Jacobian matrix of model (1) is as follows:

$$J = \begin{pmatrix} -\delta_1 B + \delta_2 T + \alpha_1 - \mu_1 & -\delta_1 C & \delta_2 C \\ \sigma_1 B & \alpha_2\left(1 - 2\frac{B}{K_B}\right) + \sigma_1 C - \sigma_2 T - \mu_2 & -\sigma_2 B \\ \frac{\theta_1 T}{T+\gamma_1} & \frac{\theta_2 T}{T+\gamma_2} & J_{33} \end{pmatrix},$$

with $J_{33} = \alpha_3 + \frac{\theta_1 C}{T+\gamma_1} - \frac{\theta_1 CT}{(T+\gamma_1)^2} - \frac{\theta_2 B}{T+\gamma_2} + \frac{\theta_2 BT}{(T+\gamma_2)^2} - \mu_3$.

a. Stability of equilibrium point for extinction of the entire state. Evaluating J at point E_0 in equation (2), we have

$$J(E_0) = \begin{pmatrix} \alpha_1-\mu_1 & 0 & 0 \\ 0 & \alpha_2-\mu_2 & 0 \\ 0 & 0 & \alpha_3-\mu_3 \end{pmatrix}.$$

The eigenvalues of matrix $J(E_0)$ are $\alpha_1-\mu_1$, $\alpha_2-\mu_2$, and $\alpha_3-\mu_3$. Hence E_0 is locally asymptotically stable if $\alpha_i < \mu_i$, $i = 1, 2, 3$.

b. Stability of biomass existence equilibrium point. Evaluating J at point E_1 in equation (3), we have

$$J(E_1) = \begin{pmatrix} \frac{K_B\delta_1}{\alpha_2}(\mu_2-\alpha_2) + \alpha_1 - \mu_1 & 0 & 0 \\ -\frac{K_B\sigma_1}{\alpha_2}(\mu_2-\alpha_2) & \mu_2-\alpha_2 & \frac{K_B\sigma_2}{\alpha_2}(\mu_2-\alpha_2) \\ 0 & 0 & \frac{K_B\theta_2}{\alpha_2\gamma_2}(\mu_2-\alpha_2) + \alpha_3 - \mu_3 \end{pmatrix}.$$

The eigenvalues of matrix $J(E_1)$ are $\frac{K_B\delta_1}{\alpha_2}(\mu_2-\alpha_2) + \alpha_1 - \mu_1$, $\mu_2-\alpha_2$, and $\frac{K_B\theta_2}{\alpha_2\gamma_2}(\mu_2-\alpha_2) + \alpha_3 - \mu_3$. Hence E_1 is locally asymptotically stable if $\alpha_i < \mu_i$, $i = 1, 3$ and $\alpha_2 > \mu_2$.

c. Stability of CO_2 and biomass equilibrium point. Evaluating J at point E_2 in equation (4), we have

$$J(E_2) = \begin{pmatrix} 0 & J_{12} & J_{13} \\ \frac{\sigma_1}{\delta_1}(\alpha_1-\mu_1) & \frac{\alpha_2}{K_B\delta_1}(\mu_1-\alpha_1) & \frac{\sigma_2}{\delta_1}(\mu_1-\alpha_1) \\ 0 & 0 & J_{33} \end{pmatrix},$$

with

$J_{12} = \frac{\delta_1}{\sigma_1}(\alpha_2-\mu_2) + \frac{\alpha_2}{K_B\sigma_1}(\mu_1-\alpha_1)$,

$J_{13} = \frac{\delta_2}{\sigma_1}(\mu_2-\alpha_2) + \frac{\alpha_2\delta_2}{K_B\delta_1\sigma_1}(\alpha_1-\mu_1)$,

$J_{33} = \frac{\theta_2}{\delta_1\gamma_2}(\mu_1-\alpha_1) + \frac{\theta_1}{\sigma_1\gamma_1}(\mu_2-\alpha_2) + \frac{\theta_1\alpha_2}{K_B\delta_1\sigma_1\gamma_1}(\alpha_1-\mu_1) + \alpha_3 - \mu_3$.

The eigenvalues of matrix $J(E_2)$ is $g = \frac{\theta_2}{\delta_1\gamma_2}(\mu_1-\alpha_1) + \frac{\theta_1}{\sigma_1\gamma_1}(\mu_2-\alpha_2) + \frac{\theta_1\alpha_2}{K_B\delta_1\sigma_1\gamma_1}(\alpha_1-\mu_1) + \alpha_3 - \mu_3$ and the remaining are the roots of the following equation.

$$g^2 + a_1 g + a_2 = 0, \tag{9}$$

with

$a_1 = \frac{\alpha_2}{K_B\delta_1}(\alpha_1-\mu_1)$,

$a_2 = \frac{\sigma_1}{\delta_1}(\alpha_1-\mu_1)\left[\frac{\delta_1}{\sigma_1}(\mu_2-\alpha_2) + \frac{\alpha_2}{K_B\sigma_1}(\alpha_1-\mu_1)\right]$.

Based on existence of E_2 in equation (4), it's clear that $a_1 > 0$ and $a_2 > 0$. Hence by Routh-Hurwitz criterion, the roots of equation (9) have negative real part and it's ensure that the eigenvalues are negative. Hence E_2 is locally asymptotically stable if $g < 0$.

d. Stability of CO_2 and temperature equilibrium point. Evaluating J at point E_3 in equation (5), we have

$$J(E_3) = \begin{pmatrix} 0 & J_{12} & J_{13} \\ 0 & J_{22} & 0 \\ \frac{\theta_1}{\delta_2\gamma_1+\mu_1-\alpha_1}(\mu_1-\alpha_1) & -\frac{\theta_2}{\delta_2\gamma_1+\mu_1-\alpha_1}(\mu_1-\alpha_1) & J_{33} \end{pmatrix},$$

with

$J_{12} = \frac{\delta_1}{\delta_2\theta_1}(\alpha_3-\mu_3)(\delta_2\gamma_1+\mu_1-\alpha_1)$,

$J_{13} = \frac{1}{\theta_1}(\mu_3-\alpha_3)(\delta_2\gamma_1+\mu_1-\alpha_1)$,

$J_{22} = \frac{\sigma_1}{\delta_2\theta_1}(\mu_3-\alpha_3)(\delta_2\gamma_1+\mu_1-\alpha_1) + \frac{\sigma_2}{\delta_2}(\alpha_1-\mu_1) + \alpha_2 - \mu_2$,

$J_{33} = -\frac{1}{\delta_2\gamma_1+\mu_1-\alpha_1}(\mu_1-\alpha_1)(\mu_3-\alpha_3)$.

The eigenvalues of matrix $J(E_3)$ are $g_1 = \frac{\sigma_1}{\delta_2\theta_1}(\mu_3-\alpha_3)(\delta_2\gamma_1+\mu_1-\alpha_1) + \frac{\sigma_2}{\delta_2}(\alpha_1-\mu_1) + \alpha_2 - \mu_2$ and the others are the roots of the following equation.

$$g^2 + b_1 g + b_2 = 0, \tag{10}$$

with

$b_1 = \frac{1}{\delta_2\gamma_1+\mu_1-\alpha_1}(\mu_1-\alpha_1)(\mu_3-\alpha_3)$,

$b_2 = \frac{\delta_2\gamma_1+\mu_1-\alpha_1}{\delta_2\gamma_1}(\alpha_3-\mu_3)$.

Based on existence of E_3 in equation (5), it's clear that $b_1 > 0$ and $b_2 < 0$. Hence by Routh-Hurwitz criterion, E_3 is not stable.

e. Stability of biomass and temperature equilibrium point. Evaluating J at point E_4 in equation (6), we have

$$J(E_4) = \begin{pmatrix} J_{11} & 0 & 0 \\ J_{21} & J_{22} & -\frac{K_B\sigma_2(\gamma_2\sigma_2+\alpha_2-\mu_2)(\alpha_3-\mu_3)}{K_B\sigma_2\theta_2+\alpha_2(\alpha_3-\mu_3)} \\ J_{31} & J_{32} & \frac{(\alpha_2\gamma_2(\alpha_3-\mu_3)+K_B\theta_2(\mu_2-\alpha_2))(\mu_3-\alpha_3)}{K_B\theta_2(\gamma_2\sigma_2+\alpha_2-\mu_2)} \end{pmatrix},$$

with

$J_{11} = \frac{K_B\delta_1(\gamma_2\sigma_2+\alpha_2-\mu_2)(\mu_3-\alpha_3)}{K_B\sigma_2\theta_2+\alpha_2(\alpha_3-\mu_3)} + \frac{\delta_2(K_B\theta_2(\alpha_2-\mu_2)+\gamma_2\alpha_2(\mu_3-\alpha_3))}{K_B\sigma_2\theta_2+\alpha_2(\alpha_3-\mu_3)} + \alpha_1 - \mu_1$,

$J_{21} = \frac{K_B\sigma_1(\gamma_2\sigma_2+\alpha_2-\mu_2)(\alpha_3-\mu_3)}{K_B\sigma_2\theta_2+\alpha_2(\alpha_3-\mu_3)}$,

$J_{22} = -\frac{\alpha_2(\gamma_2\sigma_2+\alpha_2-\mu_2)(\alpha_3-\mu_3)}{K_B\sigma_2\theta_2+\alpha_2(\alpha_3-\mu_3)}$,

$J_{31} = \frac{\theta_1(K_B\theta_2(\mu_2-\alpha_2)+\alpha_2\gamma_2(\alpha_3-\mu_3))}{K_B\theta_2(\mu_2-\alpha_2)+\alpha_2(\gamma_1-\gamma_2)(\mu_3-\alpha_3)-K_B\theta_2\sigma_2\gamma_1}$,

$J_{32} = -\frac{\alpha_2\gamma_2(\mu_3-\alpha_3)+K_B\theta_2(\alpha_2-\mu_2)}{K_B(\gamma_2\sigma_2+\alpha_2-\mu_2)}$.

The eigenvalues of matrix $J(E_4)$ are $f = \frac{K_B\delta_1(\gamma_2\sigma_2+\alpha_2-\mu_2)(\mu_3-\alpha_3)}{K_B\sigma_2\theta_2+\alpha_2(\alpha_3-\mu_3)} + \frac{\delta_2(K_B\theta_2(\alpha_2-\mu_2)+\gamma_2\alpha_2(\mu_3-\alpha_3))}{K_B\sigma_2\theta_2+\alpha_2(\alpha_3-\mu_3)} + \alpha_1 - \mu_1$ and the remaining are the roots of the following equation.

$$f^2 + c_1 f + c_2 = 0, \tag{11}$$

with

$$c_1 = \frac{\alpha_2(\gamma_2\sigma_2+\alpha_2-\mu_2)(\alpha_3-\mu_3)}{K_B\sigma_2\theta_2+\alpha_2(\alpha_3-\mu_3)} + \frac{(\alpha_2\gamma_2(\mu_3-\alpha_3)+K_B\theta_2(\alpha_2-\mu_2))(\mu_3-\alpha_3)}{K_B\theta_2(\gamma_2\sigma_2+\alpha_2-\mu_2)},$$

$$c_2 = - \frac{\alpha_2(\gamma_2\sigma_2+\alpha_2-\mu_2)(\alpha_3-\mu_3)(\alpha_2\gamma_2(\mu_3-\alpha_3)+K_B\theta_2(\alpha_2-\mu_2))(\alpha_3-\mu_3)}{(K_B\sigma_2\theta_2+\alpha_2(\alpha_3-\mu_3))K_B\theta_2(\gamma_2\sigma_2+\alpha_2-\mu_2)} - \frac{K_B\sigma_2(\gamma_2\sigma_2+\alpha_2-\mu_2)(\alpha_3-\mu_3)(\alpha_2\gamma_2(\mu_3-\alpha_3)+K_B\theta_2(\alpha_2-\mu_2))}{(K_B\sigma_2\theta_2+\alpha_2(\alpha_3-\mu_3))K_B(\gamma_2\sigma_2+\alpha_2-\mu_2)}.$$

Based on existence of E_4 in equation (6), it's clear that $c_2 < 0$. Hence by Routh-Hurwitz criterion, E_4 is not stable.

f. Stability of co-existence equilibrium point. Because E_5 in equation (7) is implicit form, then the stability of this equilibrium will be reviewed through phase field simulation. Using the parameter values in Table 2, we get equilibrium point as follows:

- $E_0 = (C_0, B_0, T_0) = (0, 0, 0)$.
- $E_1 = (C_1, B_1, T_1) = (0, -2226.46, 0)$.
- $E_2 = (C_2, B_2, T_2) = (163.72, -37.45, 0)$.
- $E_3 = (C_3, B_3, T_3) = (110.36, 0, 7.92)$.
- $E_4 = (C_4, B_4, T_4) = (0, 1150.12, -30.53)$.
- $E_{5a} = (C_{5a}, B_{5a}, T_{5a}) = (410.2, 97.65, 28.58)$.
- $E_{5b} = (C_{5b}, B_{5b}, T_{5b}) = (159.69, -39.66, -0.47)$.

Hence E_1, E_2, E_4, E_{5b} are not exist. Next by taking three different initial values, First initial value. $(C, B, T) = (400, 100, 30)$, Second initial value. $(C, B, T) = (800, 500, 10)$, and Third initial value. $(C, B, T) = (100, 300, 60)$ the results of the phase field simulation in Figure 1 are obtained as follows.

Based on Figure 1 the selection of initial values affects the type of system stability. The selection of the first and third initial values causes the system to be stable towards the equilibrium point E_{5a}. While the selection of the second initial value causes the system to be asymptotically stable towards the equilibrium point E_0. Therefore, it is expected that the equilibrium point E_5 is locally stable.

2.3. Concentration number

Inspired by the basic reproduction number (R_0) used in disease models. We introduce a concept called the "Concentration Number" (R_c). This threshold quantity represents a critical level of CO_2 concentration in the atmosphere, beyond which the associated dangers become significantly more severe [17].

To calculated R_c, we employ the next-generation matrix method [20]. Considering only the "harmful" states (C and T), the matrices F (interaction terms) and V (negation of the non-interaction terms) evaluated at the biomass existence equilibrium (E_1) are given as follows.

$$F(E_1) = \begin{pmatrix} \frac{K_B\delta_1(\mu_2-\alpha_2)}{\alpha_2} & 0 \\ 0 & \frac{K_B\theta_2(\mu_2-\alpha_2)}{\alpha_2\gamma_2} \end{pmatrix}, \quad Z(E_1) = \begin{pmatrix} \mu_1-\alpha_1 & 0 \\ 0 & \mu_3-\alpha_3 \end{pmatrix}.$$

The concentration number (R_c) is defined by the spectral radius (dominant eigenvalue in magnitude) of the matrix FZ^{-1}. Therefore we obtain R_c for model (1) is given by.

$$R_c = \max\left\{\frac{K_B\delta_1(\alpha_2-\mu_2)}{\alpha_2(\alpha_1-\mu_1)}, \frac{K_B\theta_2(\alpha_2-\mu_2)}{\alpha_2\gamma_2(\alpha_3-\mu_3)}\right\}.$$

This number represents the amount of CO_2 emissions relative to the ecosystem's capacity to absorb it. If $R_c > 1$, this indicates that CO_2 emissions are at an excessive level, leading to accumulation in the atmosphere that could trigger climate change over time. Conversely, if $R_c < 1$, it means that CO_2 emissions and accumulation in the atmosphere are not considered harmful to the ecosystem.

3. Results and discussion

3.1. Parameter estimation

In this section, we estimate the value of parameter on model (1). First, we collect data from Ref. [21], which is monthly temperature in Surabaya, Indonesia based on observations from Perak 1 station in January 2020 - December 2022. In parameter estimation, we use least-squares methods with the goal is to minimize the objective function.

$$\min_{\alpha_1,\alpha_2,\alpha_3,\delta_1,\delta_2,\sigma_1,\sigma_2,\theta_1,\theta_2,\mu_1,\mu_2,\mu_3,K_B,\gamma_1,\gamma_2} \sum_{i=0}^{t_f} (T_i - Data_i)^2,$$

with t_f is the end time of the temperature data $Data_i$ $\left(i = 0, 1, 2, \ldots, t_f\right)$, as well $T_i\left(i = 0, 1, 2, \ldots, t_f\right)$ is the numerical solutions of temperature compartment. Next we set the initial compartment such as $(C_0; B_0; T_0) = (400; 100; 29.2)$. Based on the parameter estimation results, the comparison Mean Absolute Percentage Error between the data and the model solution is 1.73%. Then we present the result of estimation and parameters value in Figure 2 and Table 2.

3.2. Sensitivity analysis

In this section, we identify the parameters that have the greatest impact on the concentration number through sensitivity analysis. We use the method described in Ref. [22] to quantify the sensitivity index as a measure of sensitivity analysis associated with the parameters. This is calculated by

$$\Upsilon_a^{R_c} = \frac{\partial R_c}{\partial a} \times \frac{a}{R_c}.$$

with a is the parameter being evaluated.

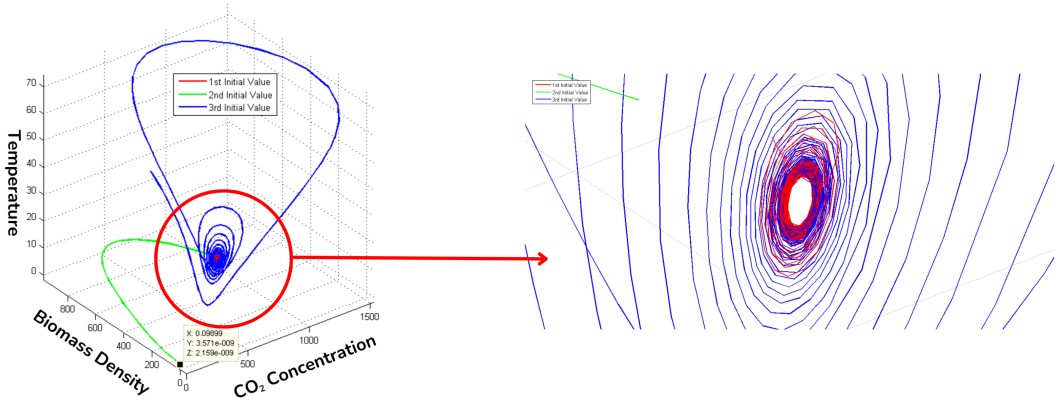

Figure 1: Phase field diagram.

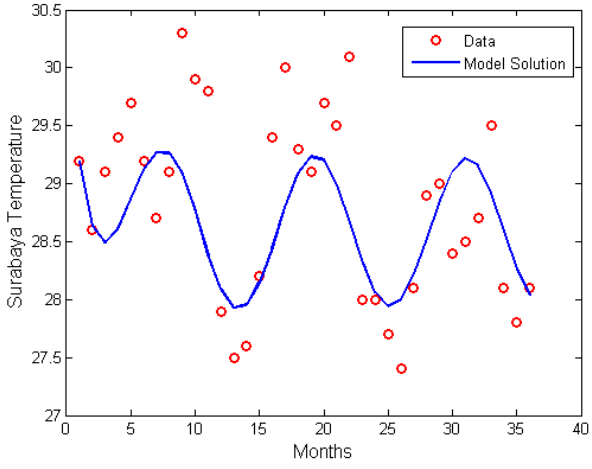

Figure 2: Parameters estimation result.

Table 2: Estimated parameters value.

Parameters	Value	Parameters	Value
α_1	0.3765	θ_1	0.0465
α_2	0.0359	θ_2	0.0157
α_3	0.0636	μ_1	0.5001
K_B	100	μ_2	0.8352
δ_1	0.0033	μ_3	0.6639
δ_2	0.0156	γ_1	0.6260
σ_1	0.0048	γ_2	0.4541
σ_2	0.0397		

Table 3: Estimated parameters value.

Parameters	Sensitivity Index for R_{c1}	Parameters	Sensitivity Index for R_{c2}
K_B	1	K_B	1
α_2	$-\frac{\mu_2}{\mu_2-\alpha_2} = -1.045$	α_2	$-\frac{\mu_2}{\mu_2-\alpha_2} = -1.045$
μ_2	$\frac{\mu_2}{\mu_2-\alpha_2} = 1.045$	μ_2	$\frac{\mu_2}{\mu_2-\alpha_2} = 1.045$
α_1	$\frac{\alpha_1}{\mu_1-\alpha_1} = 3.046$	α_3	$\frac{\alpha_3}{\mu_3-\alpha_3} = 0.106$
μ_1	$-\frac{\mu_1}{\mu_1-\alpha_1} = -4.046$	μ_3	$-\frac{\mu_3}{\mu_3-\alpha_3} = -1.106$
δ_1	1	θ_2	1
		γ_2	-1

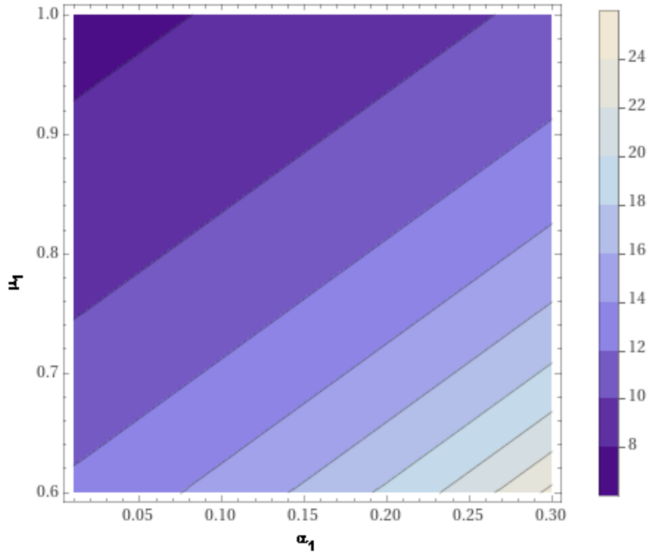

Figure 3: Contour plot of α_1 and μ_1 on the changes in R_{c1}.

Next, since R_c consists of two parts, we denote it as follows

$$R_{c1} = \frac{K_B\delta_1(\alpha_2-\mu_2)}{\alpha_2(\alpha_1-\mu_1)} \quad \text{and} \quad R_{c2} = \frac{K_B\theta_2(\alpha_2-\mu_2)}{\alpha_2\gamma_2(\alpha_3-\mu_3)}.$$

We evaluate the sensitivity index of each parameter present in R_{c1} and R_{c2} by substituting the parameter values from Table 2. The results of this sensitivity index are presented in Table 3.

Based on Table 3, the positive sign of index shows that when the values of the parameter are raised, the value of R_c will increase as well. Conversely, the negative sign of index shows that when the value of the parameter are raised, the value of R_c will decreased. The largest and smallest index from sensitivity index shows the most influential parameters on changes in R_c are α_1 and μ_1. Next, to observe the influence of α_1 and μ_1 on the changes in R_{c1}, a contour plot simulation is presented in Figure 3.

Table 4: Estimated parameters value.

Strategy	Optimal Controls	Objective Function
1	u_1^*	6.3058×10^5
2	u_2^*	5.8326×10^5
3	u_1^* and u_2^*	5.8280×10^5

Table 5: Comparison of ICER for each intervention strategies.

Strategies	Optimal Controls	Total Temperature Averted	Total Cost	ICER	ICER Recalculated
1	u_1^*	0.31	6.3058×10^5	2.03×10^6	-
2	u_2^*	86.75	5.8326×10^5	−547.43	6723.46
3	u_1^* and u_2^*	87.66	5.8280×10^5	−505.49	−505.49

Furthermore, since α_1 and μ_1 are the most influential parameters, a simulation was conducted to observe the changes in these parameter values and their effects on the populations of concentration of CO_2 (C) and photosynthetic biomass density (B) with the results presented in Figure 4.

3.3. Future climate trends

In this section, we conduct simulation using model (1) to analyze future climate trends in Surabaya, utilizing parameter values obtained from Table 2. These simulations provide insights into the projected levels of concentration of CO_2, biomass density, and atmospheric temperature in the future. Thus, the results of this simulation can serve as an important tool for policymakers in developing effective strategies to address climate change. In this simulation, we extend the time frame to $t = 150$ months to enhance the visibility of fluctuations in the graphs. This longer duration allows for a clearer representation of trends and variations over time. The results of this simulation are presented in Figure 5.

Based on Figure 5, the concentration of CO_2, biomass density, and atmospheric temperature in Surabaya exhibit a periodic pattern with a slight decreasing trend over time. Projections for the future indicate that the CO_2 concentration is expected to range from 400 to 420 ppm, reflecting the ongoing impact of greenhouse gas emissions. Additionally, biomass density is estimated to be between 92 and 102 kg/m^3, indicating the potential of the local ecosystem to absorb carbon dioxide and support environmental sustainability. Meanwhile, atmospheric temperature is projected to range from 28.1 to 29.1 degrees Celsius.

3.4. Optimal control problem

In this section, we applied optimal control strategy of the mathematical model of temperature change (1). Two control variables are implemented, namely u_1 as limiting access to private vehicles to pressure people to switch to public transportation thereby reducing CO_2 in the air from private vehicles. and u_2 as reforestation with aims to increase the natural absorption

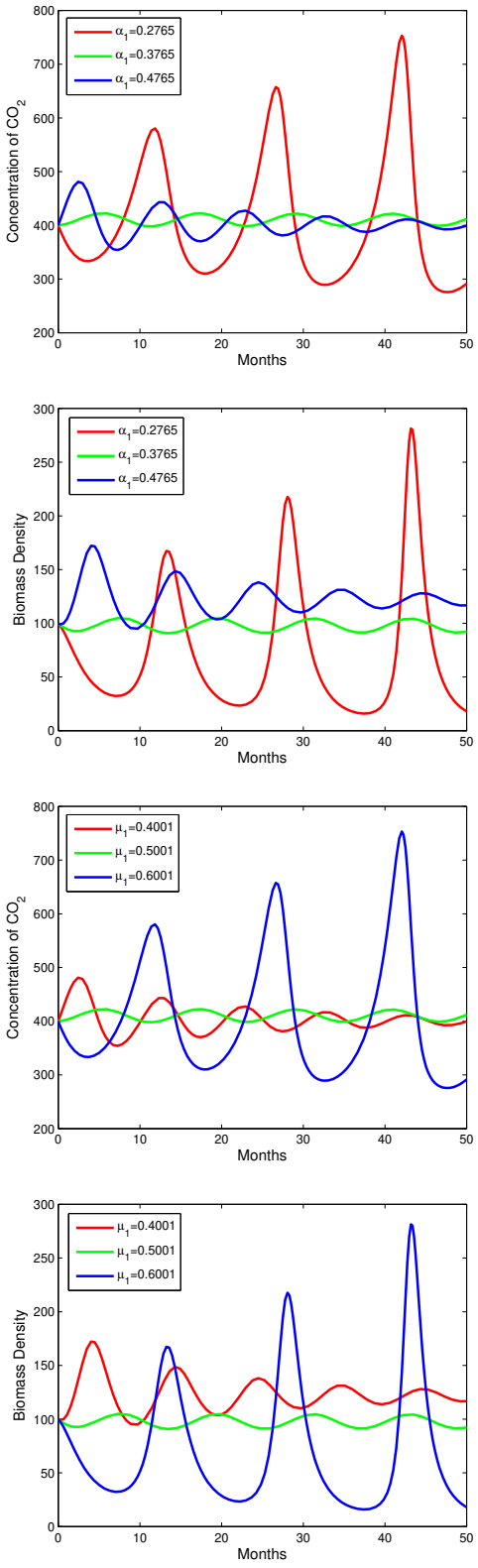

Figure 4: Simulation of the changes in α_1 and μ_1 on the populations of C and B.

of CO_2. The mathematical model of temperature change with

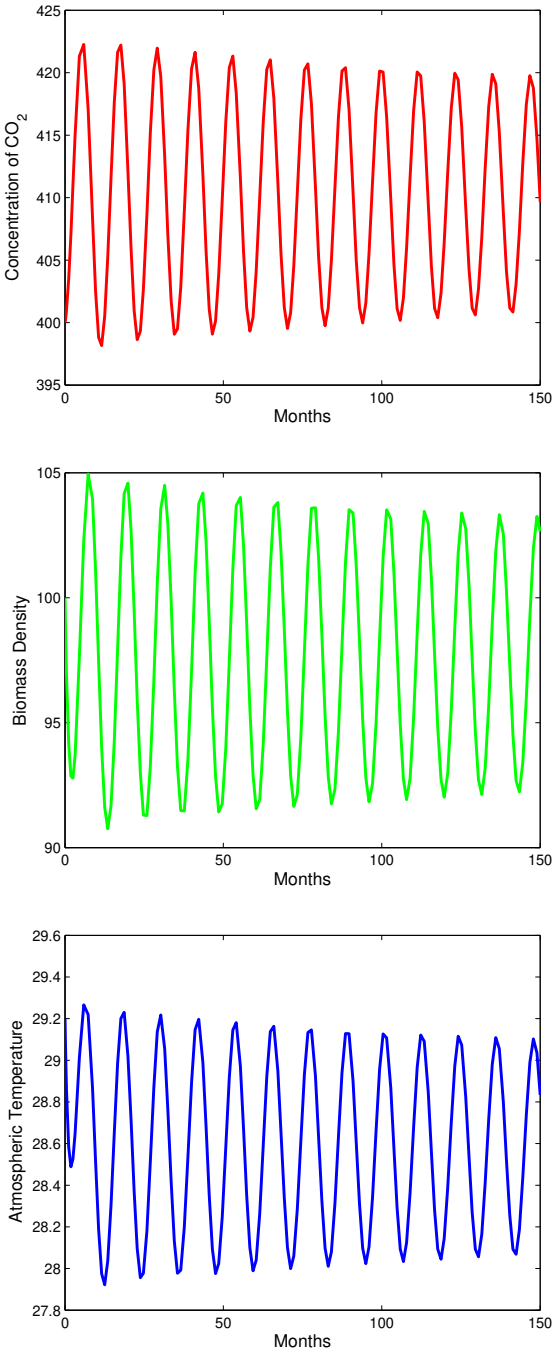

Figure 5: Simulation of future climate trend.

control variables is presented as.

$$\begin{aligned}
\frac{dC}{dt} &= \alpha_1 C - \delta_1 CB + \delta_2 CT - \mu_1 C - \psi_1 u_1 C,\\
\frac{dB}{dt} &= \alpha_2 B\left(1 - \frac{B}{K_B}\right) + \sigma_1 CB - \sigma_2 BT - \mu_2 B + \psi_2 u_2 B, \quad (12)\\
\frac{dT}{dt} &= \alpha_3 T + \frac{\theta_1 CT}{T+\gamma_1} - \frac{\theta_2 BT}{T+\gamma_2} - \mu_3 T.
\end{aligned}$$

The control function u_1 and u_2 are defined on interval $\left[0, t_f\right]$,

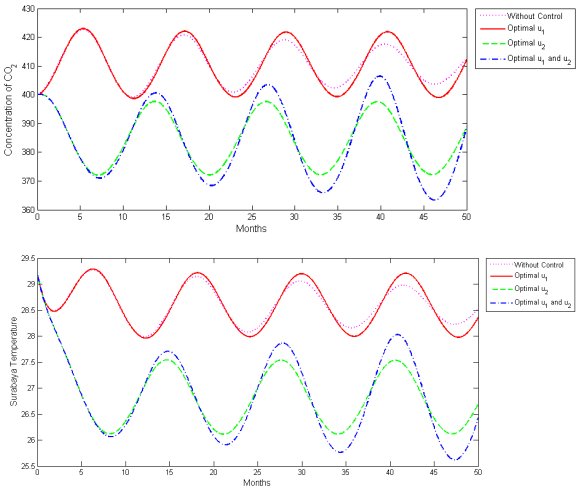

Figure 6: Optimal control result on CO_2 concentration and temperature variables.

with $0 \le u_i(t) \le 1$, $t \in \left[0, t_f\right]$, $i = 1, 2$, and t_f denotes the end time of the controls. Our goal is to minimize the concentration of CO_2 and atmospheric temperature, also the cost of applying restrictions on private vehicle access and reforestation controls as low as possible. For this, we consider the objective function

$$J(u_1, u_2) = \int_0^{t_f} \left(A_1 C + A_2 T + \frac{1}{2} C_1 u_1^2 + \frac{1}{2} C_2 u_2^2\right) dt, \quad (13)$$

where A_1, A_2, and A_3 are weights of the objective function for C and T respectively, C_1 and C_2 are weight parameters for restrictions on private vehicle access and reforestation respectively. We use the quadratic cost function for J to describe the cost of control efforts. This quadratic function can describe a nonlinear cost increase related to the implementation of control efforts in the field.

In this study, the aim of the optimal control problem is to determine the controls u_1 and u_2 so that

$$J(u_1^*, u_2^*) = \min J(u_1, u_2). \quad (14)$$

Then to solve this optimal control problem, we use Pontryagin's Maximum Principle [23]. By Pontryagin's method, we transform Eqs. (12)-(14) into the problem of minimizing the Hamiltonian function H is given by

$$H = A_1 C + A_2 T + \frac{1}{2} C_1 u_1^2 + \frac{1}{2} C_2 u_2^2 + \lambda_1 \frac{dC}{dt} + \lambda_2 \frac{dB}{dt} + \lambda_3 \frac{dT}{dt}, \quad (15)$$

with λ_i, $i = 1, 2, 3$ are called adjoint or co-state variables respect to the state variables C, B, and T.

The optimal solutions of u_1 and u_2 are obtained from solving $\frac{\partial H}{\partial u_i} = 0, i = 1, 2$. Hence, we have the control characterizations

$$u_1^* = \min\left\{1, max\left(0, \frac{\lambda_1 \psi_1 C}{C_1}\right)\right\},$$

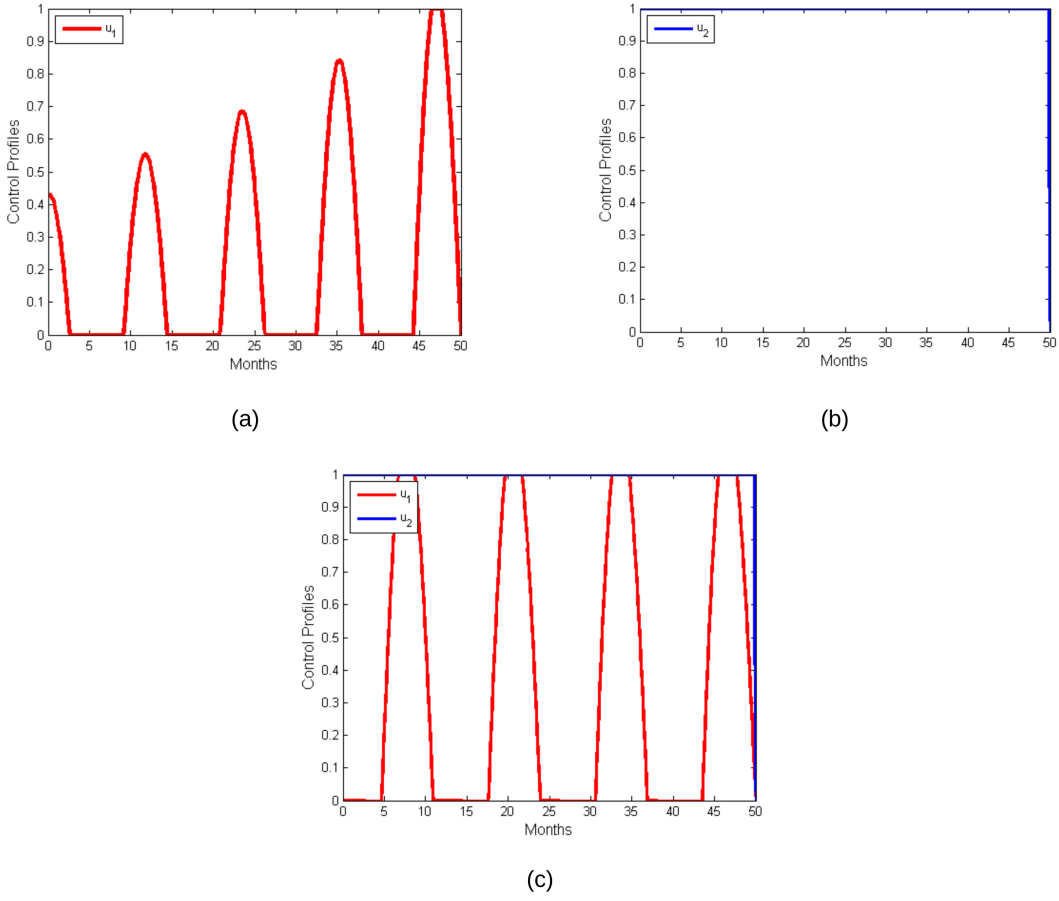

Figure 7: Control profile of (a) strategy 1, (b) strategy 2 and (c) strategy 3.

$$u_2^* = \min\left\{1, max\left(0, -\frac{\lambda_2\psi_2 B}{C_2}\right)\right\}.$$

The co-state equations is obtained by solving the set equations $\dot{\lambda_1} = -\frac{\partial H}{\partial C}, \dot{\lambda_2} = -\frac{\partial H}{\partial B}, \dot{\lambda_3} = -\frac{\partial H}{\partial T}$ such that yield

$$\begin{aligned}
\dot{\lambda_1} &= -A_1 + \lambda_1\left(-\alpha_1 + \delta_1 B - \delta_2 T + \mu_1 + \psi_1 u_1\right) + \lambda_2\left(-\sigma_1 B\right) \\
&\quad + \lambda_3\left(-\frac{\theta_1 T}{T+\gamma_1}\right), \\
\dot{\lambda_2} &= \lambda_1\left(\delta_1 C\right) + \lambda_2\left(-\alpha_2 + 2\frac{\alpha_2 B}{K_B} - \sigma_1 C + \sigma_2 T + \mu_2 - \psi_2 u_2\right) \\
&\quad + \lambda_3\left(\frac{\theta_2 T}{T+\gamma_2}\right), \\
\dot{\lambda_3} &= -A_2 + \lambda_1\left(-\delta_2 C\right) + \lambda_2\left(\sigma_2 B\right) \\
&\quad + \lambda_3\left(-\alpha_3 - \frac{\theta_1 C\gamma_1}{(T+\gamma_1)^2} + \frac{\theta_2 B\gamma_2}{(T+\gamma_2)^2} + \mu_3\right),
\end{aligned}$$

with the transversality conditions $\lambda_i\left(t_f\right) = 0,\ i = 1, 2, 3.$

By assuming $A_1 = A_2 = 100$, $C_1 = 150$, $C_2 = 10$, $\psi_1 = 0.002$, $\psi_2 = 0.05$, and the other parameters are refer to Table 2, we solve the numerical optimal control simulation using backward and forward sweep as described in Ref. [24]. We then obtained the optimally of the model, which is comparised of the model without control, the adjoint system and the optimality conditions. To ascertain which strategy or combination gives the efficient methods of controlling temperature, we considered the following strategies for our simulation, Strategy 1. Single intervention: use of restrictions on private vehicle access only ($u_2 = 0$), Strategy 2. Single intervention: use of reforestation only ($u_1 = 0$), and Strategy 3. Double intervention: combination of restrictions on private vehicle access and reforestation. The result of simulation of comparison C and T variables without and with control also the control profile of each strategy present on Figures 6 and 7.

Next, the objective function value of each strategy is presented in Table 4

3.5. Cost effectiveness analysis

In this section we evaluates and compares the benefits and the costs associated with control measures for each strategy that has been implemented in the previous section using the Incremental Cost-Effectiveness Ratio (ICER) with formula as follows.

$$\text{ICER} = \frac{\text{Difference in cost produced by strategies } i \text{ and } j}{\text{Difference in temperature averted by strategies } i \text{ and } j}.$$

ICER is used to compare 2 different strategies, namely i and j. The ICER numerator (where applicable) the differences in in-

tervention cost and avoided temperature cost while the dominator is difference in temperature outcomes. We compute the cost of a strategy as objective function in Table 4. When comparing 2 or more competing intervention strategies incrementally, one intervention is compared with the next-less-effective alternative in increasing order of total temperature averted [25, 26]. The result ICER calculation in Table 5.

The ICER indexes, as reported in Table 5, are obtained as follows.

$$\text{ICER}\,(1) = \frac{6.3058 \times 10^5 - 0}{0.31 - 0} = 2.03 \times 10^6,$$
$$\text{ICER}\,(2) = \frac{5.8326 \times 10^5 - 6.3058 \times 10^5}{86.75 - 0.31} = -547.43,$$
$$\text{ICER}\,(3) = \frac{5.8280 \times 10^5 - 5.8326 \times 10^5}{87.66 - 86.75} = -505.49.$$

Comparing Strategy 1 and Strategy 2, the use of Strategy 2 is cost saving over strategy 1. This indicate the Strategy 1 is less effectiveness and more costly than the other strategy. Hence, Strategy 1 is removed. Furthermore we recalculation the index of ICER as follows.

$$\text{ICER}\,(2) = \frac{5.8326 \times 10^5 - 0}{86.75 - 0} = 6723.46,$$
$$\text{ICER}\,(3) = \frac{5.8280 \times 10^5 - 5.8326 \times 10^5}{87.66 - 86.75} = -505.49.$$

Comparing Strategy 2 and Strategy 3, the use of Strategy 3 is cost saving over Strategy 2. This indicate the Strategy 2 is less effectiveness and more costly than the other strategy. Hence, Strategy 2 is removed. Our result suggest that Strategy 3 is the most cost-effective intervention associated with the incremental cost-effectiveness ratio (ICER).

4. Conclusion

We constructed a Lotka-Volterra model of climate change to explore the temperature in Surabaya city, Indonesia. A mathematical model consisting of three compartments is proposed in this study to describe the impacts of climate change characterized by increasing level of carbon dioxide, atmospheric temperatures and its adverse effects on living things. From the model analysis, we obtained six equilibria, namely extinction, biomass existence, coexistence of CO_2 and biomass, coexistence of CO_2, biomass, and temperature that are locally asymptotically stable with conditions, while coexistence of biomass and temperature, coexistence CO_2 and temperature are unstable. The developed dynamic model was then implemented on monthly temperature data in Surabaya City, Indonesia from January 2020 to December 2022. Based on the parameter estimation and model simulation, we predict that CO_2 concentration is expected to range from 400 to 420 ppm, biomass density is estimated to be between 92 and 102 kg/m^3, and atmospheric temperature is projected around 28.1^{o}C −29.1^{o}C in Surabaya. Furthermore, the results of the sensitivity analysis suggest the most influential parameters affecting changes in concentration number are intrinsic rate of accumulation of CO_2 and natural reduction rate of CO_2.

Next, we extended the model by incorporate two the control variables to assess the impact of three different strategies on our proposed model. Using the cost effectiveness analysis, we conclude that implementing control in the form of limiting access to private vehicles and reforestation is the best strategy to make the temperature better and cost efficiency. This study not only contributes to the theoretical understanding of the dynamics between concentration of CO_2, photosynthetic biomass density and atmospheric temperature but also offers practical policy recommendations aimed at mitigating the adverse impacts of climate change by integrating ecological and economic considerations. Future research could improve climate models by including fractional derivatives, epidemic modeling, and chaotic dynamics. Memory effects are highlighted in research on fractional epidemic models [27, 28] , which is important for long-term climate predictions, while mutual impact modeling [29, 30] enhances climate interaction analysis. Furthermore, chaotic attractors and fractal-fractional operators [31] provide insights into complex climate dynamics, enabling more effective control tactics.

Data availability

All relevant data are within the manuscript.

Acknowledgment

This work was supported by WUACD, Airlangga Community Development Grant and Matching-Fund 2023.

References

[1] Intergovernmental Panel on Climate Change (IPCC), Climate Change 2021: The Physical Science Basis, 2021. [Online]. https://www.ipcc.ch/report/ar6/wg1/.

[2] I. A. Anazonwu & M. Z. Fahmi, “Wastewater treatment, greenhouse gas emissions, and our environment”, Recent Advances in Natural Sciences **2** (2024) 121. https://doi.org/10.61298/rans.2024.2.2.121.

[3] R. Latha, K. Kakshminarayanachari & C. Bhaskar, “An analytical model for point source pollutants in an urban area with mesoscale wind and wet deposition”, Journal of the Nigerian Society of Physical Sciences **6** (2024) 2116. https://doi.org/10.46481/jnsps.2024.2116.

[4] Food and Agriculture Organization of the United Nations (FAO), “The state of the World’s forests 2020: Forests, biodiversity and people”, 2020. [Online]. https://www.fao.org/state-of-forests/en/.

[5] World Wildlife Fund (WWF), “Forest pathways report 2023”, 2023. [Online]. https://www.worldwildlife.org/publications/forest-pathways-report-2023.

[6] I. A. Pratiwi, E Prasetyo & H. D. Ardiansyah, “Greenhouse gas (GHG) emission reduction model in Surabaya”, Ecology, Environment and Conservation Paper **26** (2020) 1342. https://www.envirobiotechjournals.com/issues/article_abstract.php?aid=10785&iid=316&jid=3.

[7] U. F. Kurniawati, C. Susetyo & P. T. Setyasa, “Institutional assesment through climate and disaster resilience initiative in Surabaya”, IOP Conf. Series: Earth and Environmental Science **562** (2020) 012025. https://iopscience.iop.org/article/10.1088/1755-1315/562/1/012025.

[8] H. A. Biswas, T. Rahman & N. Haque, “Modeling the potential impacts of global climate change in Bangladesh: an optimal control approach”, Journal of Fundamental and Applied Sciences **8** (2016) 1. http://dx.doi.org/10.4314/jfas.v8i1.1.

[9] S. Mandal, Md. S. Islam & Md. H. A. Biswas, "Modeling the potential impact of climate change in living beings near coastal areas", Modeling Earth Systems and Environment **7** (2021) 1783. https://doi.org/10.1007/s40808-020-00897-5.

[10] E. A. D. Kurniawan, Fatmawati & Miswanto, "Modeling of global warming effect on the melting of polar ice caps with optimal control analysis", AIP Conference Proceedings **2329** (2021) 040006. https://doi.org/10.1063/5.0042360.

[11] S. Mandal, Md. S. Islam, Md. H. A. Biswas & S. Akter, "Modeling the optimal mitigation of potential impact of climate change on coastal ecosystems", Heliyon **7** (2021) e07401. https://doi.org/10.1016/j.heliyon.2021.e07401.

[12] S. Soldatenko, A. Bogomolov & A. Ronzhin, "Mathematical modelling of climate change and variability in the context of outdoor ergonomics", Mathematics **9** (2021) 2920. https://doi.org/10.3390/math9222920.

[13] A. Din, F. M. Khan, Z. U. Khan, A. Yusuf & T. Munir, "The mathematical study of climate change model under nonlocal fractional derivative", Partial Differential Equations in Applied Mathematics **5** (2022) 100204. https://doi.org/10.1016/j.padiff.2021.100204.

[14] P. U. Achimugwu, M. N. Kinyanjui & D. M. Malonza, "Mitigation of climate change due to excessive carbon dioxide emission and accumulation: a mathematical model approach", Communications in Mathematical Biology and Neuroscience **2023** (2023) 70. https://doi.org/10.28919/cmbn/8027.

[15] A. Sangwan, S. Choudhary, V. Anand, N. Kumar, A. Kumar, M. K. Jat & R. Ahmed, "A mathematical model for temperature-reducing potential of urban greenspaces", Earth Science Informatics **16** (2023) 4199. https://doi.org/10.1007/s12145-023-01166-6.

[16] K. L. Atoyev & P. S. Knopov, "Mathematical modeling of climate change impact on relationships of economic sectors", Cybernetics and Systems Analysis **59** (2023) 535. https://doi.org/10.1007/s10559-023-00589-9.

[17] F. O. Ochieng, "A novel data-driven dynamical model for predicting future climate trends", Modeling Earth Systems and Environment **10** (2024) 4599. https://doi.org/10.1007/s40808-024-02021-3.

[18] I. Shahid, R. A. Naqvi, M. Yousaf, A. M. Siddiqui & A. Sohail, "Controlling carbon emissions through modeling and optimization: addressing an earth system and environment challenge", Modeling Earth Systems and Environment **10** (2024) 6003. http://dx.doi.org/10.1007/s40808-024-02096-y.

[19] S. Kutala, H. Awari, S. Velu, A. Anthonisamy, N. J. Bathula & S. Inthiyaz, "Hybrid deep learning-based air pollution prediction and index classification using an optimization algorithm", AIMS Environmental Science **11** (2024) 551. https://doi.org/10.3934/environsci.2024027.

[20] P. van den Driessche & J. Watmough, "Reproduction numbers and subthreshold endemic equilibria for compartemental models of disease transmission", Mathematical Biosciences 180 (2002) 29. https://doi.org/10.1016/s0025-5564(02)00108-6.

[21] Satu Data, Statistik Sektoral Kota Surabaya Tahun 2021-2023, 2021-2023. [Online]. https://satudata.surabaya.go.id/statistik-sektoral.

[22] N. Chitnis, J. M. Hyman & J. M. Cushing, "Determining important parameters in the spread of malaria through the sensitivity analysis of a mathematical model", Bulletin of Mathematical Biology **70** (2008) 1272. https://doi.org/10.1007/s11538-008-9299-0.

[23] L. S. Pontryagin, *The Mathematical Theory of Optimal Processes*, CRC Press, Boca Raton, USA, 1987. https://api.pageplace.de/preview/DT0400.9781351433075_A37629368/preview-9781351433075_A37629368.pdf.

[24] S. Lenhart & J. T. Workman, *Optimal Control Applied to Biological Models*, Chapman and Hall/CRC, Boca Raton, USA, 2007. https://doi.org/10.1201/9781420011418.

[25] B. Buonomo & R. D. Marca, "Optimal bed net use for a dangue disease model with mosquito seasonal pattern", Mathematical Methods in the Applied Sciences **41** (2017) 573. https://doi.org/10.1002/mma.4629.

[26] Fatmawati, C. W. Chukwu, R. T. Alqahtani, C. Alfiniyah, F. F. Herdicho & Tasmi, "A Pontryagin's maximum principle and optimal control model with cost-effectiveness analysis of the COVID-19 epidemic", Decision Analytics Journal **8** (2023) 100273. https://doi.org/10.1016/j.dajour.2023.100273.

[27] S. S. Musa, S. Zhao, I. Abdulrashid, S. Qureshi, A. Colubri & D. He, "Evaluating the spike in the symptomatic proportion of SARS-CoV-2 in China in 2022 with variolation effects: a modeling analysis", Infectious Disease Modelling **9** (2024) 601. https://doi.org/10.1016/j.idm.2024.02.005.

[28] D. Baleanu, S. Qureshi, A. Yusuf, A. Soomro & M. S. Osman, "Bi-modal COVID-19 transmission with Caputo fractional derivative using statistical epidemic cases", Partial Differential Equations in Applied Mathematics **10** (2024) 100732. https://doi.org/10.1016/j.padiff.2024.100732.

[29] P. A. Naik, B. M. Yeolekar, S. Qureshi, M. Yeolekar & A. Madzvamuse, "Modeling and analysis of the fractional-order epidemic model to investigate mutual influence in HIV/HCV co-infection", Nonlinear Dynamics **112** (2024) 11679. https://doi.org/10.1007/s11071-024-09464-9.

[30] A. Padder, L. Almutairi, S. Qureshi, A. Soomro, A. Afroz, E. Hincal & A. Tassaddiq, "Dynamical analysis of generalized tumor model with Caputo fractional-order derivative", Fractal and Fractional **7** (2023) 258. https://doi.org/10.3390/fractalfract7030258.

[31] A. Atangana & S. Qureshi, "Modeling attractors of chaotic dynamical systems with fractal–fractional operators", Chaos, Solitons & Fractals **123** (2019) 320. https://doi.org/10.1016/j.chaos.2019.03.003.